www.medscape.com

Meningeal Contribution to Migraine Pain

A Magnetic Resonance Angiography Study

Sabrina Khan; Faisal Mohammad Amin; Casper Emil Christensen; Hashmat Ghanizada; Samaira Younis; Anne Christine Rye Olinger; Patrick J. H. de Koning; Henrik B. W. Larsson; Messoud Ashina

Brain. 2019;142(1):93-102.

Abstract and Introduction

Abstract

The origin of migraine pain is unknown but possibly implicates the dura mater, which is pain sensitive in proximity to the meningeal arteries. Therefore, subtle changes in vessel calibre on the head pain side could reflect activation of dural perivascular nociceptors that leads to migraine headache. To test this hypothesis, we measured circumference changes of cranial arteries in patients with cilostazol-induced unilateral migraine without aura using 3 T high resolution magnetic resonance angiography. The middle meningeal artery was of key interest, as it is the main supply of the dura mater. We also measured the superficial temporal and external carotid arteries as additional extracranial segments, and the middle cerebral, the cerebral and cavernous parts of the internal carotid ($ICA_{cerebral}$ and $ICA_{cavernous}$), and the basilar arteries as intracranial arterial segments. Magnetic resonance angiography scans were performed at baseline, migraine onset, after sumatriptan, and ≥27 h after migraine onset. Thirty patients underwent magnetic resonance angiography scans, of which 26 patients developed unilateral attacks of migraine without aura and were included in the final analysis. Eleven patients treated their migraine with sumatriptan while the remaining 15 patients did not treat their attacks with analgesics or triptans. At migraine onset, only the middle meningeal artery exhibited greater circumference increase on the pain side (0.24 ± 0.37 mm) compared to the non-pain side (0.06 ± 0.38 mm) ($P = 0.002$). None of the remaining arteries revealed any pain-side specific changes in circumference ($P > 0.05$), but exhibited bilateral dilation. Sumatriptan constricted all extracerebral arteries ($P < 0.05$). In the late phase of migraine, we found sustained bilateral dilation of the middle meningeal artery. In conclusion, onset of migraine is associated with increase in middle meningeal artery circumference specific to the head pain side. Our findings suggest that vasodilation of the middle meningeal artery may be a surrogate marker for activation of dural perivascular nociceptors, indicating a meningeal site of migraine headache.

Introduction

Migraine is a highly prevalent neurological disorder, ranked as the third highest cause of disability under age 50 and affecting some one billion people globally (Steiner *et al.*, 2016). Migraine is generally considered a neurovascular headache with intricate pathophysiological connections between deep brain structures and the trigeminal pain pathways (Olesen *et al.*, 2009). While the brain is largely insensate, stimulation of dura mater near its arteries in humans produces pain that resembles migraine headache as well as migraine-like associated symptoms of nausea and photophobia (Penfield and McNaughton, 1940; Ray and Wolff, 1940). In conjunction with this finding, preclinical models have further suggested that activation of trigeminal nerve fibres innervating the dura mater may play a key role in migraine pain. This concept is based on assays that have demonstrated that stimulating the dura mater or trigeminal ganglion with inflammatory, chemical or electrical mediators results in plasma protein extravasation, mast cell degranulation, and dilation of meningeal blood vessels (Markowitz *et al.*, 1987; Buzzi and Moskowitz, 1990; Buzzi *et al.*, 1991; Dimitriadou *et al.*, 1991; Kurosawa *et al.*, 1995; Strassman *et al.*, 1996; Levy *et al.*, 2007). These physiological responses are mediated by neuropeptides, including vasoactive calcitonin gene-related peptide (CGRP), released from activated trigeminal sensory neurons (Goadsby *et al.*, 1988; Zagami *et al.*, 1990). Further, Bolay and colleagues (2002) suggested that cortical spreading depression might also activate meningeal nociceptors by causing a persistent dural vasodilation and plasma protein extravasation. Interestingly, preclinical models have also demonstrated that acute and preventive migraine treatment can modulate the activation of dural trigeminal afferents. Notably, sumatriptan and dihydroergotamine pretreatment reduced plasma protein extravasation (Buzzi and Moskowitz, 1990; Buzzi *et al.*, 1991), a CGRP-antagonist and sumatriptan treatment blocked the increase in meningeal blood flow (Kurosawa *et al.*, 1995; Williamson *et al.*, 1997), and topiramate attenuated dural vasodilation (Akerman and Goadsby, 2005).

In the absence of directly measuring trigeminal activation within the dura mater in humans, we can measure vasodilation as a constituent of the physiological response to trigeminal activation. Here, the middle meningeal artery (MMA) is of particular interest as it is the major blood supply of the dura, richly innervated by trigeminal sensory afferents (Mayberg *et al.*, 1984). Even subtle changes in MMA calibre during migraine attacks could indicate release of vasoactive peptides from activated dural trigeminal nerve endings, ultimately initiating the pain pathway of migraine (Jacobs and Dussor, 2016).

In the present study, we applied high resolution 3 T magnetic resonance angiography (MRA) to investigate the early circumference change of cranial arteries in unilateral attacks of migraine without aura. We propose that any changes in circumference can be considered a surrogate marker for activation of dural trigeminal perivascular nociceptors. We used the highly effective phosphodiesterase-3-inhibitor cilostazol as an experimental migraine trigger (Guo *et al.*, 2014). We hypothesized that during unilateral attacks of migraine without aura, intra- and extracranial arteries exhibit ipsilateral dilation, reflecting activation of perivascular nociceptors. Also, we hypothesized that therapeutic use of the selective migraine abortive drug, sumatriptan, a 5-hydroxytryptamine agonist, would reverse this activation.

Materials and Methods

Study Design and Participants

Patients were eligible for inclusion if they were female aged 18–50 years and had a verified diagnosis of migraine without aura as defined by the International Headache Society classification (Headache Classification Committee of the International Headache Society (IHS), 2013). Patients were eligible for inclusion if they reported their spontaneous migraine to be unilateral in ≥70% of attacks. All patients were prescreened with cilostazol, and only patients who developed a migraine-like attack after the first cilostazol induction were included in the study. Exclusion criteria included any other type of headache (apart from episodic tension-type headache ≤5 days per month), any previous serious somatic or psychiatric condition, pregnant or nursing females, drug misuse, daily intake of medication (apart from oral contraceptives), or contraindications for MRI (i.e. any type of metal implantation in the body or claustrophobia). The present study is part of a larger parent protocol (protocol H-15005669, clinicaltrials.gov identifier NCT02549898), where several other parameters were recorded with MRI to be published elsewhere. Exclusion criteria specific for the parent MRI protocol also included history of atopic or drug allergy, evidence of iron overload assessed by biochemical detection of ferritin, transferrin, iron and haemoglobin, and genetic screening for haemochromatosis with the *HFE* gene. All patients underwent a full medical examination and pregnancy testing.

All patients provided written informed consent to participate in the study. The Ethical Committee for Capital Region of Denmark approved the study, which was conducted in accordance with the Helsinki Declaration of 1964 with later revisions.

Data Acquisition and Imaging Protocols

All patients reported to the clinic migraine-free for at least 5 days, and headache-free for at least 3 days. Coffee, tea, cocoa, alcohol, other methylxanthine-containing beverages, and tobacco were not allowed for at least 12 h before study start. Patients first underwent a baseline MRA (baseline scan). Upon completion of this first scan, all patients ingested 200 mg cilostazol (Pletal®, Otsuka Pharmaceutical Europe Ltd.) orally. MRA was performed again (early attack scan) after 4 h. Headache intensity and characteristics were recorded every hour from cilostazol ingestion on a verbal rating scale from 0–10 (0, no headache; 1; very mild headache; 10, worst imaginable headache). After the early attack scan, 12 of 30 patients were allocated to treat their migraine attack with 6 mg subcutaneous injection of sumatriptan (Imigran®, GlaxoSmithKline). These patients underwent an additional MRA 1 h after sumatriptan treatment (sumatriptan scan). Those patients who did not treat their attack with sumatriptan were permitted to treat their headache with only promethazine and metoclopramide, in order to exclude any direct drug effect on the cerebral vasculature. As part of the parent study design, participating patients received an iron oxide contrast agent after their early attack respective sumatriptan scan, and reported back to the clinic the next day and underwent a late MRA (late attack scan, Figure 1).

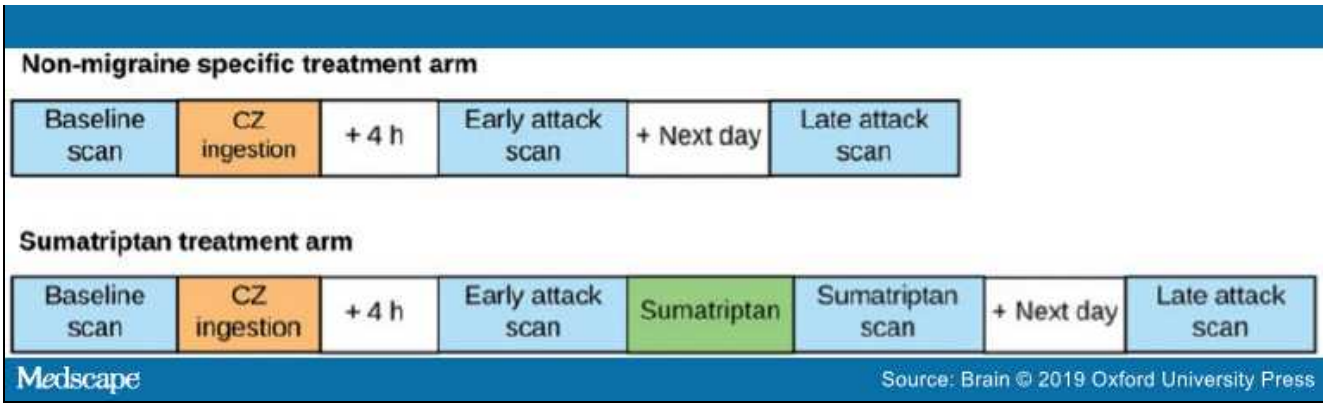

Figure 1.

Study procedures for patients who underwent MRA with or without receiving sumatriptan treatment.

MRA was performed on a 3 T Philips Achieva Scanner (Philips Medical Systems) using a 32-channel phased-array head coil. A scout MRA was performed to plan the subsequent high resolution MRA, using field of view 200 × 200 × 74 mm^3, acquired matrix size 800 × 408, acquired voxel resolution 0.25 × 0.49 × 1.00 mm^3, reconstructed voxel resolution 0.20 × 0.20 × 0.50 mm^3, repetition time 25 ms, echo time 3.5 ms, flip angle 20°, SENSE p reduction 2, four chunks, total scan duration 9 min 4 s.

Data Analysis

Baseline, early attack and sumatriptan scans. After acquisition, MRA scans were transferred to a separate workstation in DICOM format, and analysed with the LKEB-MRA vessel wall analysis software program, which has previously been applied in similar studies (Asghar *et al.*, 2011; Amin *et al.*, 2014) and has demonstrated inter- and intra-observer variation below 5% (Amin *et al.*, 2014). The program provides automated contour detection and quantification of the luminal boundaries every 0.2 mm perpendicular to the centre line in the chosen vessel segment. The investigators (S.K., C.E.C. and F.M.A.) reviewed the chosen segment and for each vessel a segment with no branches was selected to ensure the most reliable measurement. The same segment was chosen within each subject between scans and days. If the vessel segment displayed too many side branches or too curved a pattern to provide reliable circumference estimation, the measurement was excluded from the analysis.

We performed measurements on intracranial and extracranial vessels. The intracranial arteries were further classified as cerebral or extracerebral. The cerebral vessels included the middle cerebral artery (MCA), the cerebral part of internal carotid artery ($ICA_{cerebral}$), and basilar artery. The cavernous part of the internal carotid artery ($ICA_{cavernous}$) served as an extracerebral artery. The extracerebral vessels included the MMA, the superficial temporal artery (STA), and the external carotid artery (ECA). We identified MCA by marking the branch from the main trunk of the ICA. We identified $ICA_{cerebral}$ by setting the starting point in MCA and measuring caudally from where ICA branches into MCA and the anterior cerebral artery. The basilar artery segment was identified by using the point at which the two vertebral arteries conjoin as a reference. We identified the start of $ICA_{cavernous}$ by the point where ICA enters the intracranial cavity (prior to entering the cavernous sinus). The MMA was identified by marking the branch from the main trunk of the maxillary artery (or in some cases directly from the ECA), and STA and ECA were identified as either side of where the maxillary artery branches off from ECA.

Investigators who performed MRA analyses (S.K., F.M.A., and C.E.C.) were masked to patients' headache laterality.

Explorative late attack scan analyses. As part of the parent study design, participating patients received an intravenous iron oxide contrast agent after their early attack respective sumatriptan scan (Figure 1), and underwent a late attack scan on the next day. Iron oxides exhibit a relatively long intravascular phase, for which reason the late attack MRA demonstrated both intra- and extravascular enhancement, in some cases segmentally contorting the lumen boundaries detected by the LKEB-MRA vessel wall analysis software program. Because of this technical caveat of the late attack MRA, we analysed data for this specific scan exploratively. If extravascular tissue or small side branches were included due to effects of contrast enhancement, we manually corrected the measurement if possible. If not possible, the measurement was excluded from the dataset. For the late attack scan, we included three vessels; the MCA, $ICA_{cavernous}$, and MMA.

Statistical analysis. Sample size was calculated for the parent study. We calculated our sample size based on detection of at least 20% change in arterial wall thickness between the pain side and non-pain side during attack, at 5% significance (two-tailed) and with 80% power. The estimated standard deviation of arterial wall thickness changes was assumed to be 16%. Based on these assumptions, we calculated that 10 patients should be included, but increased our sample size to 30 for increased confidence in our findings.

All absolute values are presented as mean ± standard deviation (SD). Per cent changes are reported as mean and 95% confidence intervals (CI). Headache score is presented as median with interquartile range (IQR).

The primary endpoints of the study were (i) difference in circumference change of cranial arterial segments between the pain side and the non-pain side during unilateral migraine attacks; and (ii) difference in circumference change of cranial arterial segments between the pain side and the non-pain side during unilateral migraine attacks after sumatriptan treatment.

We tested for absolute differences in arterial circumference between baseline, attack, and treatment conditions and for possible side-to-side differences between the pain side and the non-pain side using the paired *t*-test. We made no adjustment for multiple analyses.

Data from the late attack scan were studied exploratively and mean circumference change of the vessels is presented on line graphs. We used SPSS (version 23.0) for all statistical analyses. All *P*-values were two-sided and considered significant if <0.05.

Data Availability

The data that support the findings of this study are available from the corresponding author, upon reasonable request.

Results

Thirty female patients underwent the complete MRA scan protocol, of whom 26 fulfilled the criteria of migraine without aura at the time of the early attack scan (Figure 2 and). The remaining four patients did not fulfill migraine without aura criteria and were excluded from the analysis.

Table 1. Clinical characteristics of migraine attacks in 26 patients prior to early attack and sumatriptan scans

	Reported characteristics
Median headache intensity (IQR)[a]	5 (3.0)
Headache laterality, right/left	12/14
Headache quality, pulsating/pressing/both	21/3/2
Nausea, yes/no	14/12
Photophobia, yes/no	23/3
Phonophobia, yes/no	18/8
Median headache intensity before sumatriptan (IQR)[b]	7 (2)
Median headache intensity after sumatriptan (IQR)[b]	3 (4)

[a]Verbal rating scale 0–10.
[b]Data missing for two patients, *n* = 9.

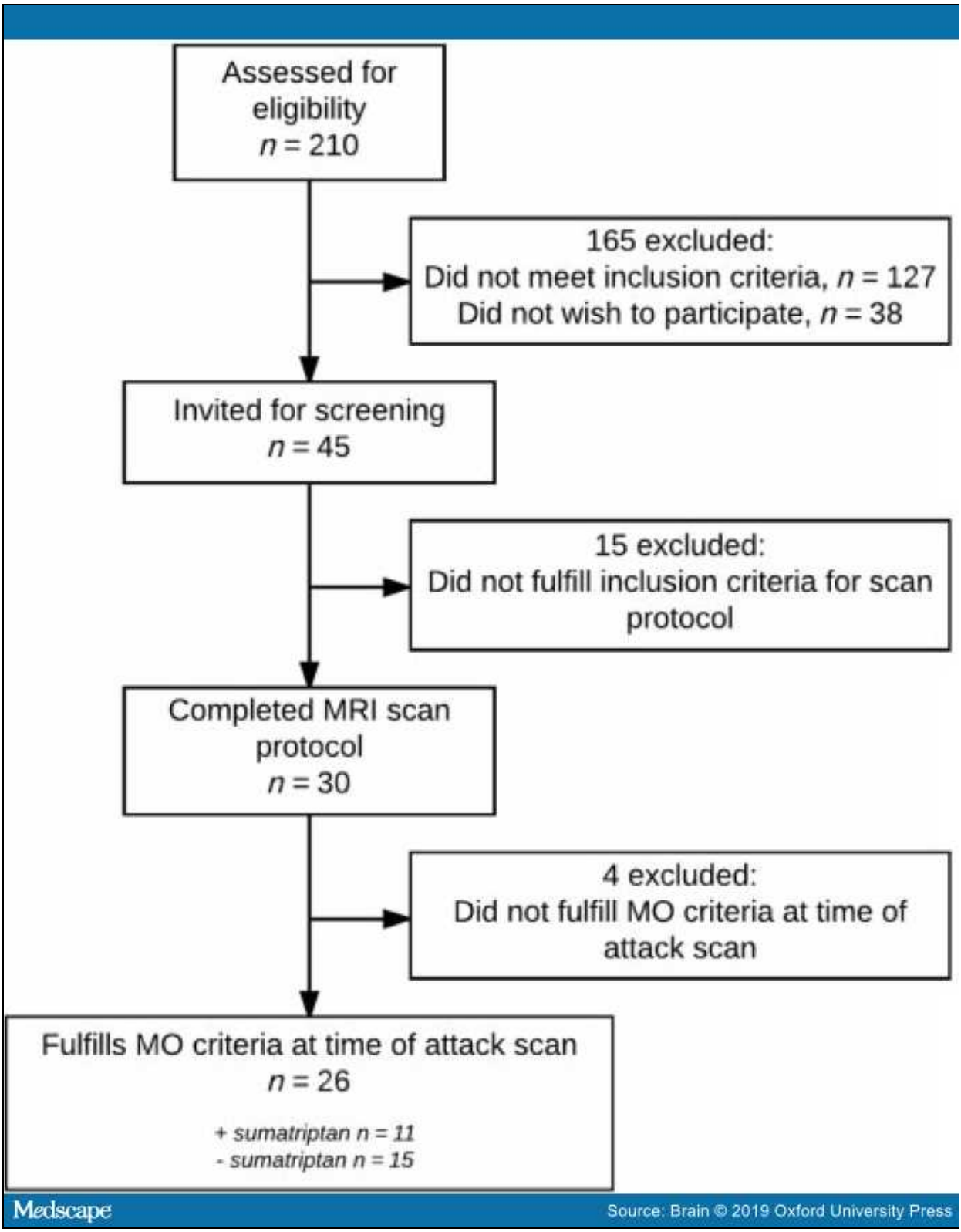

Figure 2.

Flowchart of study inclusion process. MO = migraine without aura.

Median time from migraine onset to early attack scan ranged from within 1 h after onset to maximum 4 h after onset. All 26 included patients fulfilled the ICHD-3 criteria of migraine without aura (Headache Classification Committee of the International Headache Society (IHS), 2013) at the fixed time of the early attack scan.

After the early attack scan, 11 of 26 patients received treatment with 6 mg subcutaneous sumatriptan, and underwent an additional scan 1 hour (range 25 min to 1 h) after treatment. The remaining 15 patients treated their attacks with promethazine and metoclopramide.

All 26 patients also underwent a late attack scan, median 30 h (range 28–33) after migraine onset for patients treated with sumatriptan, and median 28 h (range 27–33) after migraine onset for patients who did not treat with sumatriptan ().

Table 2. Clinical characteristics of 26 migraine patients prior to late attack scan

	Reported characteristics at late attack scan
Median time from migraine onset to late scan (range)	
Treated with sumatriptan, *n* = 11	30 h (28–33)
Not treated with sumatriptan, *n* = 15	28 h (27–33)
Number of patients with ongoing headache at time of late scan, yes/no	13/13
Number of patients who experienced diffuse headache at any time point between early and late scan, yes/no[a]	12/13
Median time from last report of headache to late scan (range)[a]	2 h (0–20.75)
Number of patients who fulfilled MO criteria at last headache report, yes/no[a]	9/16
Median headache intensity at last headache report (IQR)	1 (2)

[a]Data missing for one patient, *n* = 25.
MO = migraine without aura.

Eighteen of 26 patients (69%) reported unilateral headache and eight (31%) reported bilateral headache with a predominant pain side. We tested for side-to-side differences in circumference of all investigated arterial segments at baseline, and found no difference between the pain and non-pain sides ($P > 0.05$).

Circumference Changes During the Early Migraine Attack

We found a unilateral increase in the circumference of MMA on the pain side, 5.23 ± 0.57 mm, compared to baseline, 5.00 ± 0.50 mm ($P = 0.005$) (Figure 3). There was no difference in MMA circumference on the non-pain side, 5.13 ± 0.43 mm, compared to baseline, 5.08 ± 0.49 mm ($P = 0.473$). Correspondingly, the circumference change on the pain side (0.24 ± 0.37 mm) was significantly larger than on the non-pain side (0.06 ± 0.38 mm) ($P = 0.002$).

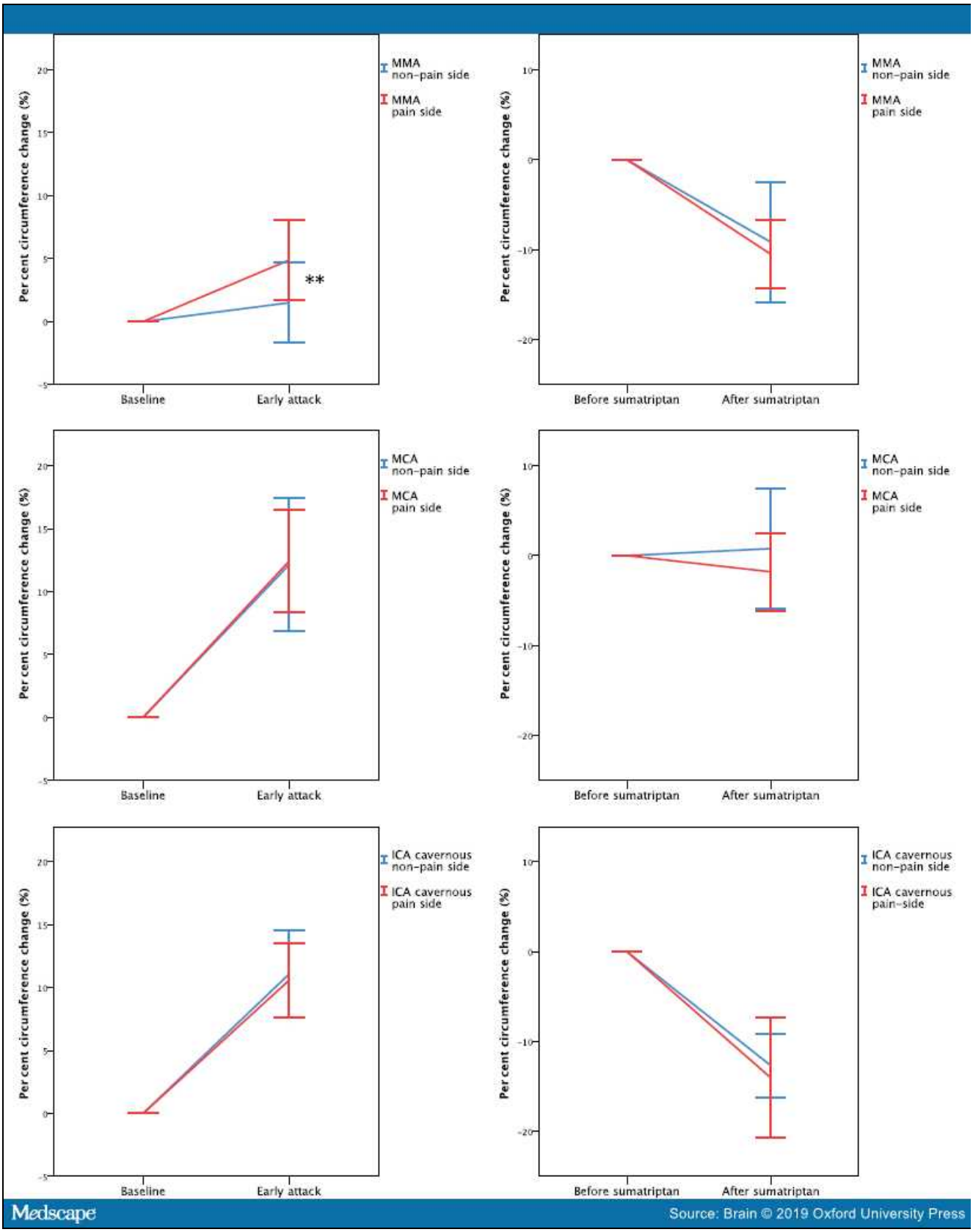
Per cent circumference change (%)
MMA non-pain side
MMA pain side
**
Baseline
Early attack
Before sumatriptan
After sumatriptan
MCA non-pain side
MCA pain side
ICA cavernous non-pain side
ICA cavernous pain side
ICA cavernous pain-side
Medscape
Source: Brain © 2019 Oxford University Press

Figure 3.

Per cent circumference change (%) and 95% CI error bars of the middle meningeal (*n* = 24), middle cerebral (*n* = 19), and the cavernous part of internal carotid artery (*n* = 24) at baseline and during early migraine attack. **Circumference change of the MMA was significantly larger on the pain side (0.24 ± 0.37 mm) compared to the non-pain side (0.06 ± 0.38 mm) (*P* = 0.002).

We found a bilateral increase in the circumference of MCA, $ICA_{cerebral}$, $ICA_{cavernous}$, and ECA compared to baseline (). The basilar artery was also dilated. Comparing the circumference change on the pain side with the non-pain side, we found no difference for any of the mentioned arteries. We found no difference in STA circumference between baseline and early migraine attack.

Table 3. Mean circumference difference on the pain and non-pain side in 26 patients with unilateral migraine attacks compared to baseline

Artery	Patients	Mean circumference difference between baseline and attack, (mm)	*P*-value
MCA			
Pain side	19	1.07 (0.74)	0.738
Non-pain side		1.03 (0.91)	
ICA cerebral			
Pain side	26	1.19 (1.07)	0.590
Non-pain side		1.13 (9.94)	
ICA cavernous			
Pain side	24	1.45 (0.99)	0.912
Non-pain side		1.43 (1.02)	
ECA			
Pain side	17	0.34 (0.62)	0.432
Non-pain side		0.45 (0.75)	
STA			
Pain side	26	0.12 (0.51)	0.946
Non-pain side		0.13 (0.44)	
MMA			
Pain side	24	0.24 (0.37)	0.002
Non-pain side		0.06 (0.38)	

Data are mean circumference change (SD). *P*-value calculated with paired *t*-test comparing mean difference between baseline and attack scan on pain and non-pain side, respectively.

Circumference Changes After Sumatriptan Treatment

Sumatriptan caused bilateral circumference reductions in MMA, $ICA_{cavernous}$, ECA and STA. There was no difference between the relative circumference reductions on the pain side compared to the non-pain side for these arterial segments (). Sumatriptan did not alter the circumference of MCA, $ICA_{cerebral}$ or the basilar artery (Figure 3).

Table 4. Mean circumference difference on the pain and non-pain side in 11 patients with unilateral migraine attack after sumatriptan compared to pretreatment

Vessel	Patients	Mean circumference difference between early attack and sumatriptan, mm	*P*-value
MCA			
Pain side	9	−0.18 (0.61)	0.468
Non-pain side		0.08 (0.90)	
ICA cerebral			
Pain side	11	−0.20 (0.95)	0.357
Non-pain side		0.19 (0.86)	
ICA cavernous			
Pain side	10	−2.30 (1.52)	0.383
Non-pain side		−1.96 (0.81)	

ECA			
Pain side	6	−1.72 (0.67)	0.605
Non-pain side		−1.59 (0.99)	
STA			
Pain side	10	−0.76 (0.57)	0.832
Non-pain side		−0.80 (0.64)	
MMA			
Pain side	9	−0.58 (0.30)	0.543
Non-pain side		−0.48 (0.45)	

Data are mean circumference change (SD). *P*-value calculated with paired *t*-test comparing mean difference between early attack and sumatriptan scan on pain and non-pain side, respectively.

Circumference Changes During the Late Migraine Attack

In patients not treated with sumatriptan, we found bilateral dilation of the MMA and $ICA_{cavernous}$ during the late attack scan, while the MCA circumference was not different from baseline. There was no difference between the pain and the non-pain side at this time point for any of the investigated arteries. Descriptive data are presented in Figure 4.

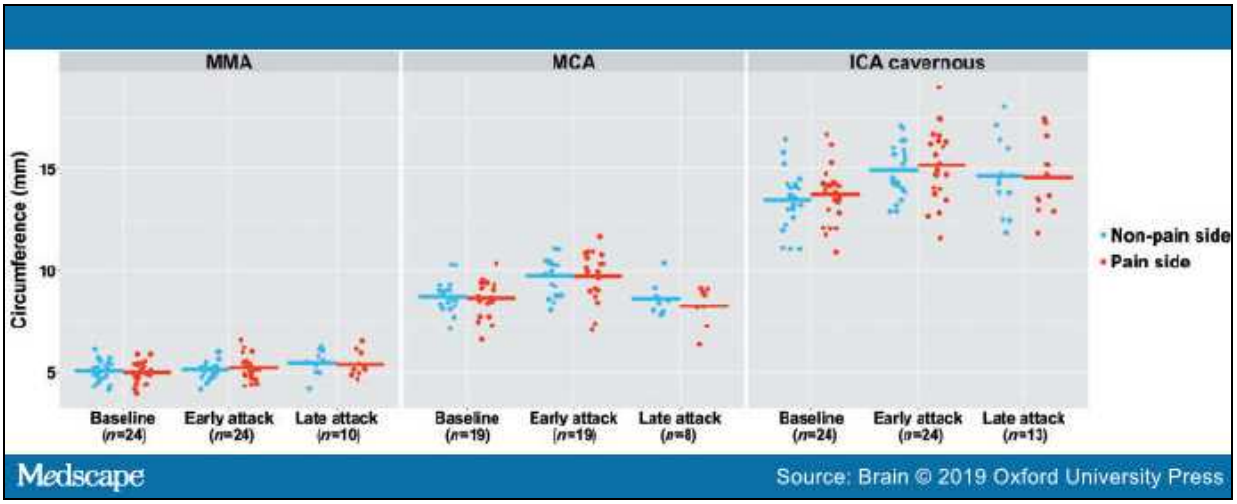

Figure 4.

Temporal evolution of circumference (mm) at baseline, early attack, and late attack of the middle meningeal, middle cerebral, and cavernous part of the internal carotid artery. Ongoing headache at time of late attack (yes/no): MMA (6/4), MCA (5/3), $ICA_{cavernous}$ (8/5). Report of bilateral headache at any time point between early and late scan (yes/no/missing data): MMA (6/4), MCA (4/3/1), $ICA_{cavernous}$ (7/5/1).

Discussion

Here, we present the earliest MRA recordings during attacks of migraine without aura. The main finding of this study was a slight dilation of MMA ipsilateral but not contralateral to the reported head pain during the onset phase of migraine. Subsequent administration of sumatriptan constricted MMA on both the pain and non-pain sides. Moreover, the first-ever exploratory investigation of intra- and extracerebral arteries in the late phase of migraine in patients not treated with migraine-specific rescue medication, suggests that MMA is subject to prolonged, bilateral dilation.

The exact role of vascular involvement in migraine has been the topic of much debate, recently fuelled by the findings of Amin and colleagues (2013), who suggested that vasodilation itself is not a principal component in migraine pain. This notion has contributed to a shift of emphasis from mechanical distension of vascular smooth muscle cells towards mechanisms related to activation and sensitization of perivascular sensory afferents in mediating migraine pain (Ashina *et al.*, 2017).

As MMA receives trigeminal innervation along its entire course (Schueler *et al.*, 2014), it is a tentative assumption that circumference changes pertaining to the extracranial MMA are a direct reflection of changes occurring around intracranial MMA. An important novel finding of this study is that MMA is the only cranial artery to increase in circumference exclusively on the pain side

during the early phase of migraine, possibly reflecting an activation of dural trigeminal nociceptors by cytochemical changes occurring in the perivascular space. This activation involves plasma protein extravasation (Markowitz *et al.*, 1987) and release of various neuropeptides including the potent vasodilator calcitonin gene-related peptide (Edvinsson and Uddman, 1981; Messlinger *et al.*, 1993).

The vasodilation observed in this study cannot be attributed to a systemic drug effect of cilostazol, as the non-pain side of MMA as well as both sides of STA did not increase in circumference. A *post hoc* power analysis revealed that with a significance level of 5%, a standard deviation of 0.24970 and sample size of 24, we would be able to detect a difference in circumference change between MMA pain and non-pain side of 0.15 mm with 80% power, and 0.17 mm with 90% power. The actual detected difference in circumference change of MMA in this study was 0.178 mm. Interestingly, STA and MMA, both extracranial arteries, receive comparable trigeminal innervation (Liu *et al.*, 2003, 2008), yet they exhibit different vascular responses in the onset phase of migraine. Considering this finding, it would further appear that MMA dilation occurring ipsilateral to the headache is suggestive of a meningeal site of migraine pain.

Sumatriptan constricted all extracerebral arteries but had no effect on the cerebral arteries (i.e. MCA or $ICA_{cerebral}$), corroborating earlier findings (Asghar *et al.*, 2011; Amin *et al.*, 2013). Apart from its vasoconstrictive properties, sumatriptan also attenuates plasma levels of CGRP during electrical stimulation of the trigeminal ganglion (Buzzi *et al.*, 1991), blocks plasma protein extravasation in dura mater (Buzzi and Moskowitz, 1990) as well as synaptic transmission between first and second order trigeminovascular neurons (Levy *et al.*, 2004), contributing to its migraine-aborting properties. The anti-nociceptive effect of sumatriptan treatment is reflected in patient-reported verbal rating scale scores, which dropped from 7 before sumatriptan to 3 after treatment.

Cilostazol crosses the cell membrane and acts intracellularly by inhibiting the phosphodiesterase-3-enzyme, resulting in an accumulation of cyclic AMP (Birk *et al.*, 2004). Interestingly, our findings show that sumatriptan blocks this intracellular effect of cilostazol in extracerebral but not intracerebral arteries.

Previous MRA Studies in Migraine

Earlier MRA studies have found varying changes in MMA calibre during migraine attacks, alternating between no dilation (Schoonman *et al.*, 2008), moderate dilation on only the pain side (Asghar *et al.*, 2011), and substantial bilateral dilation (Amin *et al.*, 2014). These discrepancies in vascular response could be attributed to difference in time from migraine onset to time of scan, as vascular changes during the migraine attack depend on time from onset to examination (Shayestagul *et al.*, 2017). Difference in time to scan could also explain our finding of slight MMA dilation on the pain side, while Asghar and colleagues (2011) reported moderate dilation of the same artery. The authors did not report time from onset of migraine to MRA; however, as our early attack scan captures the onset phase of migraine, it is possible that the full potential of MMA dilation may not have been reached at this time point.

It could also be considered that different migraine triggers induce differential vascular responses over time. CGRP provocation may induce immediate migraine attacks in 40% of patients (Guo *et al.*, 2016), whereas cilostazol only induces delayed migraine attacks (Guo *et al.*, 2014). This distinction in induction pattern could explain our finding of pain side dilation of only MMA in cilostazol-induced migraine, whereas CGRP-induced migraine leads to pain side dilation of both MMA and MCA, suggesting that the migraine cascade has evolved further along its course at a given time point after CGRP compared to cilostazol, exhibiting dilatory responses from more arteries. Another difference between CGRP and cilostazol is that the latter dilates intracerebral arteries whereas CGRP has no direct effect on the MCA (Asghar *et al.*, 2010, 2011). Therefore, a possible slight side-to-side difference of MCA calibre in our study may be hidden under a relatively large bilateral MCA dilation. Notably, pharmacological migraine triggers may vary in biochemical properties and direct comparisons of agents should consider these differences.

Late Attack Phase of Migraine

This MRA study is part of a larger parent MRI protocol, with a study design that included a late attack scan performed 1 day after onset of migraine. Data from this late phase of migraine allow us the unique assessment of vascular changes of the cranial circulation across time. The purpose of this exploratory analysis was to investigate whether dilation from the onset phase of migraine persisted into the late phase of the attack, and whether unilaterality of dilation was maintained. The three arteries of interest were chosen to represent the intracerebral (MCA), extra-cerebral ($ICA_{cavernous}$), and extracranial (MMA) circulations. The sequential circumference changes in patients who did not treat their attacks with sumatriptan suggest that MMA further dilates in the late phase of migraine, both on the pain and non-pain side that was first reported by the patients at migraine onset. $ICA_{cavernous}$maintains its circumference increase from the early attack phase, while MCA circumference decreases towards baseline.

It could be contemplated whether the persistent dilation of MMA and $ICA_{cavernous}$can be attributed to the drug effect of cilostazol. We find this highly improbable, as any drug effect would also affect MCA, which is not the case. Also, 29 h after migraine onset, the drug effect of cilostazol would have diminished greatly, considering that cilostazol reaches its maximum plasma concentration after 3 h and has a half-life of 13 h (Bramer *et al.*, 1999). Second, one could consider whether the persistent bilateral circumference increase is related to head pain, especially since the majority of investigated patients reported ongoing headache at the time of the late attack scan (Figure 4). Interestingly, >50% of patients reported a diffuse headache at some point between the early and late attack scans, despite the attack beginning as unilateral. These findings suggest that unilateral activation of perivascular nociceptors is a key characteristic of specifically the onset phase of migraine in our patients, associated with initiation of head pain. In later stages of the attack, intra- and extracranial arteries exhibit bilateral activation and sensitization of trigeminal perivascular nociceptors. This phenomenon corresponds to clinical reports from patients who experience unilateral head pain in the initial phase of their attack, which later spreads to a diffuse, bilateral head pain. Taken together, we suggest that the temporal changes of MMA circumference may be indicative of the ditto temporal evolution in migraine pain location, starting as unilateral and spreading to

diffusely bilateral. With the present data, we cannot explain the observed sustained increase in $ICA_{cavernous}$ circumference in the late phase of the migraine attack.

Because of the technicalities of performing late attack MRA analyses, only three MMA segments were eligible for analysis in patients who received sumatriptan treatment. Therefore, we cannot draw conclusions on the temporal pattern of MMA circumference changes for this patient group.

The software program applied uses the partial volume effect to achieve sub-voxel accuracy. The ratio of the signal intensity inside and outside the vessel is used to place the boundary using a variation of the full-width half-maximum (FWHM) method, as previously described by de Koning *et al.* (2003). In this work, the authors evaluated the detection method against X-ray angiography and ground truth measurements of phantoms. The method was able to accurately detect vessels that were three voxels wide (<5% error compared to ground truth). Applying this logic to our data and using the median acquired voxel size of 0.49 mm, this would correspond to a least detectable vessel circumference of 4.7 mm. The smallest MMA circumference measured in our study was 5.00 mm. The detected difference of 0.23 in MMA circumference on the pain side is under a voxel size; however, it is a mean difference measured across 24 eligible subjects for MMA analysis, where the value for each subject is a mean of up to 26 circumference values measured every 0.2 mm on a maximally 5-mm long vessel segment. Hence, we consider this detected difference a reliable measure.

Our study has a number of limitations. First, angiography analyses of the late phase migraine attack were associated with technical challenges, as blooming artefacts due to the application of iron oxide nanoparticles as contrast agent could in principle influence the visualization of arterial luminal boundaries, leading to overestimating of circumference. However, this does not explain why only MMA and $ICA_{cavernous}$, but not MCA, display dilation in the late phase of the migraine attack.

Second, as we mainly investigated the larger arteries of the brain, we cannot exclude that circumference changes also may have affected other and possibly smaller cerebral and dural arteries. However, circumference changes of the smaller cerebral arteries may alter cerebral blood flow, which does not seem to be the case in migraine without aura (Lauritzen and Olesen, 1984; Ferrari *et al.*, 1995). With regards to smaller dural arteries, we have recently examined the relationship between the large extracranial dural MMA and the smaller intracranial portion of the artery, and found similar dilation between the two segments (Christensen *et al.*, 2018). We are therefore confident that the MMA dilation found in our study may be considered representative of changes in the smaller branches of MMA in the first part of the cranial convexity.

Third, with an MRA study we can only glean circumference changes at a given time point along the continuum of pathophysiological events that occur before, during, and after a migraine attack. This fosters the question whether migraine without aura could be associated with short-lived changes in circumference, which could go unrecognized. While we cannot exclude having missed minute- or second-long calibre changes, we find this improbable considering the temporal aspect of dilation induced by vasoactive neuropeptides. An experimental migraine study demonstrated that pituitary adenylate cyclase-activating peptide-38 (PACAP-38) infusion induced prolonged vasodilation of the superficial temporal and middle meningeal arteries lasting at least 2 h (Amin *et al.*, 2014). Also, CGRP infusion was shown to cause vasodilation of the superficial temporal artery after pretreatment with placebo compared to pretreatment with the CGRP receptor antagonist olcegepant; a dilatory response that lasted from 30 to 150 min after infusion (Petersen *et al.*, 2005). Furthermore, Birk and colleagues (2004) demonstrated that cilostazol induced a reduction in MCA blood flow velocity that did not reach a plateau within the 4-h observation period. Based on the assumption that activated perivascular dural nociceptors would result in release of vasoactive peptides, including CGRP and PACAP-38, and corroborating this assumption with the presented experimental findings, we find it improbable that migraine would be associated with fleeting vasodilation.

The major novel finding of the present study is that initiation of a migraine attack is associated with increase in MMA circumference on the head pain side, suggesting activation of dural perivascular nociceptors. We propose that this headache-specific dilation of MMA precedes unilateral dilation of intracerebral arteries in the initiating cascade of migraine, suggesting a meningeal site of migraine headache.

References

1. Akerman S, Goadsby PJ. Topiramate inhibits trigeminovascular activation: an intravital microscopy study. Br J Pharmacol 2005; 146: 7–14.

2. Amin FM, Asghar MS, Hougaard A, Hansen AE, Larsen VA, de Koning PJH, et al. Magnetic resonance angiography of intracranial and extracranial arteries in patients with spontaneous migraine without aura: a cross-sectional study. Lancet Neurol 2013; 12: 454–61.

3. Amin FM, Hougaard A, Schytz HW, Asghar MS, Lundholm E, Parvaiz AI, et al. Investigation of the pathophysiological mechanisms of migraine attacks induced by pituitary adenylate cyclase-activating polypeptide-38. Brain 2014; 137: 779–94.

4. Amin FM, Lundholm E, Hougaard A, Arngrim N, Wiinberg L, de Koning PJ, et al. Measurement precision and biological variation of cranial arteries using automated analysis of 3 T magnetic resonance angiography. J Headache Pain 2014; 15: 25.

5. Asghar MS, Hansen AE, Amin FM, van der Geest RJ, Koning P van der, Larsson HBW, et al. Evidence for a vascular factor in migraine. Ann Neurol 2011; 69: 635–45.

6. Asghar MS, Hansen AE, Kapijimpanga T, van der Geest RJ, van der Koning P, Larsson HBW, et al. Dilation by CGRP of middle meningeal artery and reversal by sumatriptan in normal volunteers. Neurology 2010; 75: 1520–6.

7. Ashina M, Hansen JM, á Dunga BO, Olesen J. Human models of migraine–short-term pain for long-term gain. Nat Rev Neurol 2017; 13: 713–24.
8. Birk S, Edvinsson L, Olesen J, Kruuse C. Analysis of the effects of phosphodiesterase type 3 and 4 inhibitors in cerebral arteries. Eur J Pharmacol 2004; 489: 93–100.
9. Birk S, Kruuse C, Petersen KA, Jonassen O, Tfelt-Hansen P, Olesen J. The phosphodiesterase 3 inhibitor cilostazol dilates large cerebral arteries in humans without affecting regional cerebral blood flow. J Cereb Blood Flow Metab 2004; 24: 1352 –8.
10. Bolay H, Reuter U, Dunn AK, Huang Z, Boas DA, Moskowitz MA. Intrinsic brain activity triggers trigeminal meningeal afferents in a migraine model. Nat Med 2002; 8: 136–42.
11. Bramer SL, Forbes WP, Mallikaarjun S. Cilostazol pharmacokinetics after single and multiple oral doses in healthy males and patients with intermittent claudication resulting from peripheral arterial disease. Clin Pharmacokinet 1999; 37 (Suppl 2): 1–11.
12. Buzzi MG, Carter WB, Shimizu T, Heath H, Moskowitz MA. Dihydroergotamine and sumatriptan attenuate levels of CGRP in plasma in rat superior sagittal sinus during electrical stimulation of the trigeminal ganglion. Neuropharmacology 1991; 30: 1193–200.
13. Buzzi MG, Moskowitz MA. The antimigraine drug, sumatriptan (GR43175), selectively blocks neurogenic plasma extravasation from blood vessels in dura mater. Br J Pharmacol 1990; 99: 202–6.
14. Christensen CE, Amin FM, Younis S, Lindberg U, de Koning P, Petersen ET, et al. Sildenafil and calcitonin gene-related peptide dilate intradural arteries: A 3T MR angiography study in healthy volunteers. Cephalalgia 2018. doi: 10.1177/0333102418787336.
15. Dimitriadou V, Buzzi MG, Moskowitz MA, Theoharides TC. Trigeminal sensory fiber stimulation induces morphological changes reflecting secretion in rat dura mater mast cells. Neuroscience 1991; 44: 97–112.
16. Edvinsson L, Uddman R. Adrenergic, cholinergic and peptidergic nerve fibres in dura mater involvement in headache? Cephalalgia 1981; 1: 175–9.
17. Ferrari MD, Haan J, Blokland JA, Arndt JW, Minnee P, Zwinderman AH, et al. Cerebral blood flow during migraine attacks without aura and effect of sumatriptan. Arch Neurol 1995; 52: 135–9.
18. Goadsby PJ, Edvinsson L, Ekman R. Release of vasoactive peptides in the extracerebral circulation of humans and the cat during activation of the trigeminovascular system. Ann Neurol 1988; 23: 193–6.
19. Guo S, Olesen J, Ashina M. Phosphodiesterase 3 inhibitor cilostazol induces migraine-like attacks via cyclic AMP increase. Brain 2014; 137: 2951–9.
20. Guo S, Vollesen ALH, Olesen J, Ashina M. Premonitory and nonheadache symptoms induced by CGRP and PACAP38 in patients with migraine. Pain 2016; 157: 2773–81.
21. Headache Classification Committee of the International Headache Society (IHS). The International Classification of Headache Disorders, 3rd edition (beta version). Cephalalgia 2013; 33: 629–808.
22. Jacobs B, Dussor G. Neurovascular contributions to migraine: moving beyond vasodilation. Neuroscience 2016; 338: 130 –44.
23. de Koning PJH, Schaap JA, Janssen JP, Westenberg JJM, van der Geest RJ, Reiber JHC. Automated segmentation and analysis of vascular structures in magnetic resonance angiographic images. Magn Reson Med 2003; 50: 1189–98.
24. Kurosawa M, Messlinger K, Pawlak M, Schmidt RF. Increase of meningeal blood flow after electrical stimulation of rat dura mater encephali: mediation by calcitonin gene-related peptide. Br J Pharmacol 1995; 114: 1397–402.
25. Lauritzen M, Olesen J. Regional cerebral blood flow during migraine attacks by Xenon-133 inhalation and emission tomography. Brain 1984; 107 (Pt 2): 447–61.
26. Levy D, Burstein R, Kainz V, Jakubowski M, Strassman AM. Mast cell degranulation activates a pain pathway underlying migraine headache. Pain 2007; 130: 166–76.
27. Levy D, Jakubowski M, Burstein R. Disruption of communication between peripheral and central trigeminovascular neurons mediates the antimigraine action of 5HT 1B/1D receptor agonists. Proc Natl Acad Sci USA 2004; 101: 4274–9.
28. Liu Y, Broman J, Edvinsson L. Central projections of the sensory innervation of the rat middle meningeal artery. Brain Res 2008; 1208: 103–10.
29. Liu Y, Zhang M, Broman J, Edvinsson L. Central projections of sensory innervation of the rat superficial temporal artery. Brain Res 2003; 966: 126–33.

30. Markowitz S, Saito K, Moskowitz MA. Neurogenically mediated leakage of plasma protein occurs from blood vessels in dura mater but not brain. J Neurosci 1987; 7: 4129–36.

31. Mayberg MR, Zervas NT, Moskowitz MA. Trigeminal projections to supratentorial pial and dural blood vessels in cats demonstrated by horseradish peroxidase histochemistry. J Comp Neurol 1984; 223: 46–56.

32. Messlinger K, Hanesch U, Baumgärtel M, Trost B, Schmidt RF. Innervation of the dura mater encephali of cat and rat: ultrastructure and calcitonin gene-related peptide-like and substance P-like immunoreactivity. Anat Embryol 1993; 188: 219 –37.

33. Olesen J, Burstein R, Ashina M, Tfelt-Hansen P. Origin of pain in migraine: evidence for peripheral sensitisation. Lancet Neurol 2009; 8: 679–90.

34. Penfield W, McNaughton F. Dural headache and innervation of the dura mater. Arch Neurol Psychiatry 1940; 44: 43.

35. Petersen KA, Lassen LH, Birk S, Lesko L, Olesen J. BIBN4096BS antagonizes human alpha-calcitonin gene related peptide-induced headache and extracerebral artery dilatation. Clin Pharmacol Ther 2005; 77: 202–13.

36. Ray BS, Wolff H. Experimental studies on headache–Painsensitive structures of the head and their significance in headache. Arch Surg 1940; 41: 813–56.

37. Schoonman GG, van der Grond J, Kortmann C, van der Geest RJ, Terwindt GM, Ferrari MD. Migraine headache is not associated with cerebral or meningeal vasodilatation–a 3T magnetic resonance angiography study. Brain 2008; 131: 2192 –200.

38. Schueler M, Neuhuber WL, De Col R, Messlinger K. Innervation of rat and human dura mater and pericranial tissues in the parietotemporal region by meningeal afferents. Headache 2014; 54: 996–1009.

39. Shayestagul NA, Christensen CE, Amin FM, Ashina S, Ashina M. Measurement of blood flow velocity in the middle cerebral artery during spontaneous migraine attacks: a systematic review. Headache 2017; 57: 852–61.

40. Steiner TJ, Stovner LJ, Vos T. GBD 2015: migraine is the third cause of disability in under 50 s. J Headache Pain 2016; 17: 104.

41. Strassman AM, Raymond SA, Burstein R. Sensitization of meningeal sensory neurons and the origin of headaches. Nature 1996; 384: 560–4.

42. Williamson DJ, Hargreaves RJ, Hill RG, Shepheard SL. Sumatriptan inhibits neurogenic vasodilation of dural blood vessels in the anaesthetized rat—intravital microscope studies. Cephalalgia 1997; 17: 525–31.

43. Zagami AS, Goadsby PJ, Edvinsson L. Stimulation of the superior sagittal sinus in the cat causes release of vasoactive peptides. Neuropeptides 1990; 16: 69–75.

Funding
Lundbeck Foundation (R155-2014-171) and Novo Nordisk Foundation (NNF11OC101433 and NNF15OC0017132).

Abbreviations
CGRP = calcitonin gene-related peptide; ECA = external carotid artery; ICA = internal carotid artery; MCA = middle cerebral artery; MMA = middle meningeal artery; MRA = magnetic resonance angiography; STA = superficial temporal artery

Brain. 2019;142(1):93-102.